Bio-based PA5.10 for Industrial Applications: Improvement of Barrier and Thermo-mechanical Properties with Rice Husk Ash and Nanoclay

Bio-based PA5.10 for industrial applications: improvement of barrier and thermo-mechanical properties with rice husk ash and nanoclay

Daniele Battegazzore [a*], Alberto Frache [a]

[a] Dipartimento di Scienza Applicata e Tecnologia, Politecnico di Torino, sede di Alessandria, Viale Teresa Michel 5, 15121 Alessandria, Italy

[*]Corresponding author: Tel/Fax: +390131229343/+390131229399; e-mail address: daniele.battegazzore@polito.it

Abstract

Composites consisting of renewable PA5.10 were obtained from melt compounding with a modified clay (CL) and/or a by-product obtained from the combustion of rice husk (RHA). Two different industrialized lab-scale machines were used to obtain the final shape: a film extrusion machine and an injection moulding apparatus. The industrial application requirements for polyamides generally need good barrier properties and high thermo-mechanical strength.

Considering the barrier properties, the CL was able to decrease the oxygen permeability to less than half with respect to neat PA5.10. DMTA demonstrated that the addition of RHA caused a consistent enhancement (+46°C) in the heat deflection temperature (HDT) compared to the neat PA5.10 matrix, increasing the possible areas of interest. Furthermore, the simultaneous presence of RHA and CL provided the best result reaching an extraordinary HDT of 131°C. A complete discussion taking into account the morphology, crystallinity and filler-matrix adhesion evaluation was reported as well as comparison of performances with other bio-PAs composites.

These two fillers can therefore be used separated or together combined in PA5.10 for functional purposes in a sustainable scenario.

Keywords:

Particle-reinforced composites; Synergism; Thermomechanical properties; Injection moulding; Extrusion.

1. Introduction

Due to the growing awareness about the environmental impact, new regulations and the need of materials recycling, considerable work is underway to replace the petroleum-based plastics with those derived from renewable sources. Among all such polymers, both biodegradable such as polylactic acid, polyhydroxyalkanoates, starch and cellulose derived materials and non-biodegradable such as bio-polyethylene, bio-polyethylene terephthalate and bio-polyamides are included. The forecast data published by the European Bioplastics [1] shows how the field of use of such bio-based polymers is continuously growing. Furthermore, from the same report, it seems that the greatest increase in their production will occur for the bio-based but not biodegradable section (56.8% of the bio-plastics in 2018 [1]). Indeed, the market is looking for long-lasting application and not only for disposable materials. In this scenario, polyamides (11.6% of the bio-market in 2018 [1]) were recently evaluated by industries and literature for long-term applications [2-8]. An overview of the bio-based processes for the production of these polymers from biomass is presented by Harmsen et al. [9]. They report the bio-based building blocks (1,4-butanediamine; caprolactam, adipic acid, hexanediamine, 1,10-decanediamine, sebacic acid, 11-amino-undecanoic acid) involved in the bio-PAs industrial production processes. Other recent researches focus on the use of terpenes, terpenoids and other natural molecules but are still confined to laboratory scale [10] [11] [12]. Some of the PAs are already produced industrially (e.g. PA10.10, PA6.10, PA11) while others such as PA5.10, PA4.10, PA10.12 are still limited to industrial research or pilot plants [13, 14] [15]. In particular, the PA5.10 has the potential to be developed by combining

microbial fermentation for the production of cadaverine and polymerization of biocadaverine with sebacic acid into PA510 [13] [16].

To broaden the possible uses of these matrices, comparative studies must be carried out by using industrial equipments.

The general researches in this field focus on improving the properties and decreasing the price of these bio-polyamides for functional materials. In particular, two of their main drawbacks are their poor barrier and thermo-mechanical properties. Generally, researchers adopted the methods of polymer blending and/or addition of inorganics/fillers to improve such properties [17-20] [21] and industries also look for the economic sustainability and feasibility.

On one hand, some studies were performed on the use of renewable PAs with clays [4, 6, 18, 22, 23] that exhibited enhancements in the thermo-mechanical and barrier properties. Indeed, such fillers are able to increase the crossing path of permeating molecules and to increase the stiffness as they are more rigid than the matrices.

On the other hand, a lot of other inorganic or organic fillers could be used. The selection of organic fillers is usually limited by their thermal stability at the process temperatures. Hence, the choice in the present article is to use an inorganic by-product, the ash obtained from the combustion of the rice husk (coded as RHA). Such residue is substantially silica that comes from renewable sources (bio-silica) used directly without any chemical treatment. It is thermally stable, potentially abundant, economically sustainable and, above all, is considered a by-product dangerous for health and air pollution. This filler has been widely used as a filler in different polymers [24-29] rarely in bio-based PAs [6] and never in PA5.10.

This work aimed to use the bio-based PA5.10 for possible industrial application in the thin film or bulk object field and to investigate the barrier and thermo-mechanical properties. In order to increase such properties, PA5.10-based composites with a commercial modified nano clay (CL) and a commercially available bio-silica (RHA) were prepared and investigated. The

use of only CL was investigated to increase the barrier property of the film extruded material. The mechanical performances, with particular attention to heat deflection temperature (HDT), were compared with other bio-polyamides (PA6.10 and PA10.10) with the same fillers. The combined use of micro and nano fillers was also investigated for the bulky object to evaluate a possible synergistic effect on thermo-mechanical properties. A deep discussion with the investigation of morphology, crystallinity and quantitative filler-matrix adhesion evaluation was reported.

2. Material and methods

2.1 Materials

2.1.1 PA5.10

The Polyamide PA5.10 was produced by Radici Chimica SpA "Radilon® PX". The PA under study has only the "10" structural unit derived from renewable resources (castor oil), thus the renewable carbon content is 67 %. Nevertheless, a 100% biobased PA5.10 is industrially available based on Cathay Industrial Biotech's 100% biobased 1,5 pentamethylenediamine monomer called C-BIO N5 using sugarcane for feedstock.

2.1.2 Fillers

The natural montmorillonite modified with methyl hydrogenated tallow bis-2-hydroxyethyl quaternary ammonium (Cloisite®30B) (coded as CL) and the rice husk ash (MICRO SILICA MS 325) (coded as RHA) with a density of 2.18–2.3 g/cm³, specific surface of 15–30 m²/g and particle dimension of 325 mesh were purchased from Southern Clay Products Inc. and SB Sílica Brasil Ltda., respectively.

2.2 Composite preparation

PA5.10 was dried at 80°C for 8 h in an industrial dryer from Piovan before extrusion, reaching <200 ppm of water content, assessed by Karl-Fisher titration. Analogously, CL was dried before the extrusion process in a vacuum convection oven at 130°C for 10 h.

PA5.10 composites (Table 1) were melt blended using a co-rotating twin screw extruder LEISTRITZ ZSE 18/40 D (Figure 1). The screw speed was fixed at 300 rpm. The heating temperature was set in the eight thermostated barrel blocks from 225 to 240°C. A gravimetric feeder was used in the main hopper at the beginning of the screw for the introduction of the polymer and a second feeder for the fillers was placed in the middle of the barrel. The total extrusion output was fixed at 3 kg/h. The screw profile used is reported in previous works [6, 23]. Hereafter, the samples will be coded based on nominal compositions of fillers as reported in Table 1. The pellets obtained from the extrusion were dried at 80°C for 4 h in the same industrial dryer before the next forming process.

2.3 Film extrusion

A single screw extruder (Eurotech Extrusion Machinery S.r.l.) with a L=80cm and D=25mm was used. The molten polymers were stretched in the machine direction by a calender and finally, the resulting film was rolled on a reel (Figure 1). The parameters used are the same as already used for the other bio-PAs [23] and the barrel heating temperature was set at 220°C.

2.4 Injection moulding

Pellets obtained by extrusion were processed using an injection moulding machine Babyplast 6/10P at 220°C (Figure 1). 5A type specimens according to the standard ISO527 were prepared and used for tension tests and dynamic-mechanical thermal analyses (DMTA).

2.5 Characterization techniques

Oxygen permeability (OP) was measured by using a Multiperm ExtraSolution instrument at 23°C and 50% relative humidity with an initial conditioning time of 15 h. A film with an area equal to 50 cm^2 was placed between the two halves of the permeability chamber (Figure 1). To completely remove traces of oxygen, the film was flushed with a nitrogen flow rate of 70 ml min^{-1}. Subsequently, the gas flow in one of the two cell halves was switched to oxygen and the sample left to equilibrate. The end of the test was automatically established by the instrument when the collected data reached an oxygen transmission rate (OTR) steady-state accuracy of 0.5%. The OTR values were given by the instrument taking into account the atmospheric pressure and the OP was calculated dividing the OTR by the film thickness measured with a micrometre device.

Tensile tests were performed at room temperature (23±1°C) using a Zwick Roell Z100 machine, following the ISO 527 standard. The tensile modulus was calculated at 1 mm/min rate, then the rate was increased up to 5 mm/min until the specimen broke. The samples for stress-strain analyses were 5A type and five specimens were used for each formulation (Figure 1). The loading cell used has a maximum load of 5 kN. The average values of the tensile modulus (E), the elongation at break (ε), the maximum tensile strength (σ_{max}), the tensile strength at yield (σ_y) and corresponding standard deviations were calculated.

The Dynamic-Mechanical Thermal Analysis (DMTA) were performed using a DMA Q800 (TA Instruments) using the single cantilever clamp. The temperature scan was in the range between 30°C and 200ºC applying a heating rate of 3ºC/min, a frequency of 1 Hz and an oscillation amplitude of 0.05%. The heat deflection temperature (HDT) of composites was calculated following Takemori [30] work as the temperature at which the modulus crosses the defined value of 800 MPa that corresponds to the applied load of 1.82 MPa.

Prior to DMTA and tension tests, all specimens were conditioned at 23±1°C and 50% relative humidity in a climatic chamber till weight equilibrium was reached and for a minimum of 48 h.

The morphology of bio-composites was observed using a LEO-1450VP Scanning Electron Microscope (beam voltage: 20 kV; working distance: 15 mm). The elemental analysis was performed with an X-ray probe (INCA Energy Oxford, Cu-Kα X-ray source, k=1.540562 Å). The samples were obtained by cryomicrotome, pinned up to conductive adhesive tapes and gold-metallized.

The rheological properties were measured using an ARES rheometer fitted with a 25 mm parallel plate geometry. Tests were performed at 220°C under a nitrogen atmosphere to avoid any degradation. The sample disks for the rheometer were compression moulded at the same temperature into a 25 mm diameter hole and 1 mm thick plate. Dynamic strain sweep tests were carried out and confirmed the linearity of the viscoelastic region up to 20% strain at 100 rad/s of frequency. Furthermore, the frequency sweeps were carried out to determine the complex viscosity (η*) over the frequency range of 0.1–100 rad/s at 10% of strain.

Differential Scanning Calorimetry (DSC) analyses were performed with a Q20 TA Instruments analyzer with a single heating ramp from 25°C to 250°C at 10°C/min. The stress relaxation (ΔH_{sr}) and melting (ΔH_m) enthalpies were determined and the degree of crystallinity (χ_c) evaluated using Equation 1 [31] [23].

$$\chi_c = \frac{\Delta H_m - \Delta H_{sr}}{\Delta H_{100} \cdot (1-x)} \cdot 100$$

Equation 1

where ΔH_{100} is the melting enthalpy of the 100 % crystalline polymer matrix (244 J/g [32]) and x is the nominal filler weight percentage.

X-ray diffraction (XRD) analyses were performed with PANalytical X'Pert Pro, powered by a Philips PW3040/60 X-ray generator and fitted with a PIXcell 1d detector. Diffraction data are

acquired by exposing film extruded samples to Cu-Kα X-ray radiation, which has a characteristic wavelength (λ) of 1.5418 Å. X-rays were generated from a Cu anode supplied with 40 kV and a current of 40 mA. The data were collected over a range of 3-30° 2θ with a step size of 0.026° 2θ and nominal time per step of 100s, using the scanning PIXcell 1d detector. Fixed anti-scatter and divergence slits of 1/16° and 1/32° were used together with a beam mask of 10mm and all scans were carried out in 'continuous' mode.

2.6 Mechanical data analysis

The effect of polymer-filler interactions can be quantitatively described using Pukanszky's model for particle-based composites, as described in Equation 2 [33] and reported in previous works [6, 34]. It is employed as a simple tool to make comparisons and comments on different formulations. Specifically, Equation 2 allows to investigate a linear relationship between the natural logarithm of reduced yield stress (σ_{red}) and the filler content (φ_f).

$$\log(\sigma_{red}) = \log\frac{\sigma_c \cdot (1 + 2.5 \cdot \varphi_f)}{\sigma_m \cdot (1 - \varphi_f)} = B \cdot \varphi_f$$

Equation 2

where σ_c and σ_m are the yield stresses (σ_y) of the composite and matrix, respectively; B is a term corresponding to the load carrying capability of the filler and depends on filler-matrix interactions; φ_f is the filler volumetric fraction.

Thus, for the application of Equation 2, it is necessary to know the filler volumetric fraction (φ_f). The RHA and CL density within the composites were calculated performing weight measurements in air and water on the final composite specimens and assuming the density of PA5.10 1.07 g/cm^3. A density of 1.75, 1.74 and 1.96 g/cm^3 for the RHA, RHA-CL (ratio 2:1) and CL were found, respectively. Subsequently, these values have been used for calculating the volumetric fractions (ϕ) required by the model (0.134, 0.102, and 0.027 for PA5.10_20S, PA5.10_10S5C and PA5.10_5C, respectively).

Furthermore, the value of parameter *B* in Equation 2 increases proportionally to the degree of CL exfoliation if the other parameters remain constant as supposed by Szazdi et al. [35]. They have calculated a B factor of 1.8 for unmodified CL without any kind of exfoliation and a B factor of 195 assuming a CL complete exfoliation. By this way, is possible to calculate the extent of exfoliation applying Equation 3 [23].

$$\%\ \text{of exfoliation} = \frac{B - 1.8}{195 - 1.8} * 100$$

Equation 3

3. Results and Discussion

3.1 Permeability

One of the most important aspects for materials suitable for packaging in the film shape is the protection against oxygen. To evaluate such barrier property, the permeation of oxygen through an area of 50 cm^2 was evaluated and the average thickness measured and reported in Table 2. No data are reported for materials with RHA as filler because is not possible to obtain a thin film with this formulations.

The OP measured was 3.7±0.4 cm^3*mm/m^2*day*atm a better result than reported with other bio-PAs [23]. The dispersed CL gave an improvement (51%) in the barrier properties thanks to the increase in the tortuosity path. The reached value of 1.8 cm^3*mm/m^2*day*atm is exactly the same as obtained with PA6.10_5C and comparable with a commercial PA6 [36].

3.2 Mechanical properties

The mechanical properties of the prepared bio-composites were thoroughly investigated in tension mode. To test the film's appropriateness to be used in the packaging field, the tensile stress/strain analyses at room temperature were performed on dog-bone specimens directly obtained by punching from the extruded films (Figure 1). The collected data are listed in Table 3 and a representative curve is reported in Figure 3. On the other hand, the properties of

samples obtained by injection moulding were tested directly on 5A type specimens (Figure 1). The data are reported in the same Table 3 as well a representative curve is reported in Figure 3.

As expected, when an inorganic filler (RHA or CL) is added to a polymer matrix, a significant increase of Young's modulus and a huge decrease in the deformation at break was observed (see E and ε data in Table 3).

As far as film samples were concerned, the CL addition to PA5.10 resulted in an increase of the 45% in the modulus (E) with respect to the corresponding film matrix, a similar result was found for the same CL in PA10.10 matrix [18] [23]. Enhancements in the strength at yield (+36%) and in the maximum strength (+8%) are also reported and result better than what achieved with PA10.10 [18] [23]. These results are usually associated with good filler-matrix interaction and to a good filler dispersion/distribution. Conversely, a conspicuous reduction in the elongation at break is reported (from over 200% to 90%), generally ascribed to some agglomerated particles/fillers. The addition of RHA to PA5.10 (PA5.10_20S) caused 16% decrease in the maximum tensile strength (σ_{max}) and 2% in the strength at yield point (σ_y) when compared to the injection moulded neat matrix as well as a dramatic decrease of the ε. Despite an increase in the modulus is reported, this result is generally caused by the low efficiency of transferring stresses from the matrix to the reinforcement. This fact could be ascribed to a great dimension of particles which concentrate the stresses and to a low chemical adhesion property. Similar behaviour has been found in the literature with other PAs and different natural fillers [14] [37] [38] [39] [40].

The combination of both micro and nano-filler seems a good solution to reach balanced properties. Indeed, the sample with both RHA and CL presents intermediate strength properties, the best increase in the stiffness (E). Unfortunately, a further worsening of the elongation at break was also found. Therefore, this micro-nano solution has a synergistic

result for the stiffness, an additive behaviour for the strength and an antagonist action for the toughness.

The scatter plot reported in Figure 2 shows the tensile modulus as a function of the strength and can be useful for the correct selection of the material according to the applicative requests. In the same figure, coloured areas have also been traced. The grey area corresponds to the set containing the various PA bio-matrices. As it is possible to see, the moduli fall between 1 and 2 GPa and the strength between 30 and 60 MPa except for one sample. This range also includes one of the most common polymers from oil sources, the PP, reported in the graph as a comparison. The use of various types of fillers leads to a significant increase in the modulus, but only slight improvements in the strength. In the graph, these composites are highlighted with two areas: the red one for formulations with less than 30 wt.% of filler amount and the yellow one for quantities greater than 30 wt.%. The only cases where a substantial and simultaneous increase in both rigidity and strength are found, are included in the green area. These last composites are obtained using glass or carbon fibres, reinforcing fillers with a high aspect ratio and synthetic origin.

3.3 Thermo-mechanical analysis and HDT calculation

In addition to mechanical properties in tension mode at room temperature, the dynamic thermo-mechanical analysis (DMTA) in single cantilever mode was used to establish the effect of the filler type and temperature on the storage modulus of PA5.10 and to extrapolate the HDT. All the data are reported in Table 3 and a representative curve is plotted in Figure 4. One of the main drawbacks of several renewable polymers is their poor thermo-mechanical properties. No exception is done for the bio-PAs and also for the PA5.10. Indeed the PA5.10 HDT is found at around 62°C (Table 3), only slightly higher than PA6.10 [6], PA10.10 [39], PA11 [21]. The general increase in the modulus found by adding the fillers to the PA5.10 is

reflected in the increase of the HDT because the material is now rigid enough to remain above the 800 MPa threshold.

Thus the maximum operating temperature is accounted to 108°C in PA5.10_20S, 46°C more than the neat matrix. This impressive result is well over the already tested PA6.10 (72°C) and PA10.10 (61°C) with the same filler [6]. Similar to what already studied, the partial replacement of RHA with CL in PA5.10_10S5C further increase the HDT value of 23°C, reaching 131°C. This result is comparable to that obtained by Zierdt et al. with PA11 and 50 wt.% of beech fibres (140°C) and clearly superior to that obtained with 30 wt.% of the same filler (80°C) [21] or with 30 wt.% of wood fibre in PA11 (50°C) by Armioun et al. [40].

Considering that the addition of only CL to the matrix produces a slight increase in HDT (13°C), while the joint action with RHA gave a higher increase of 23°C, the behaviour is not just an additive effect between RHA and CL but a synergic effect.

This result is very impressive because it has never been reached with others bio-PAs and the same fillers (see Figure 4) and opens important horizons for the use of these composites in the specific high temperature areas. Better results were obtained only with synthetic fillers such as glass fibres (153°C) and carbon fibres (170°C) in PA10.10 [39] or carbon fibres in PA11 (142°C) [40] but in these cases, no bio-fillers and by-products were used.

3.4 Morphological analysis

The deep study of the morphology of composites was carried out in order to understand the structure-properties correlation.

The micrograph of PA5.10_5C sample (Figure 5) shows the presence of some isolated big agglomerates of 10 μm diameter (a) but also a huge quantity of white little dots smaller than 0.1 μm and thus sub micrometric (b).

Figure 5**c** and Figure 5**e** show two magnifications of PA5.10_20S and Figure 5**d** and Figure 5**f** of PA5.10_10S5C. The composites with 20 wt.% of RHA exhibit a homogeneous distribution and wide dispersion of particle size of silica. A contemporaneous presence of fine particles under 0.1 μm and big ones around 50 μm within the polymer matrix were detected, as already reported in previous works with the same filler [6, 41]. The hypotheses made on the filler dimensions in the mechanical characterization are therefore confirmed by the morphological analysis.

The contemporaneous presence of RHA and CL in PA5.10_10S5C substantially never change the dispersion and distribution of single particles from SEM observations. To distinguish the two fillers the elemental analyses are exploited: Si, Al, Mg elements for the CL (analyses 1, 2 and 3 in Figure 5) and Si and K for the RHA (analysis 4 in Figure 5). Therefore, the contemporary presence of CL and RHA gives some better properties to composite that are not evident from the investigated morphology through the SEM. On the other hand, the maximum load born and elongation at break properties have not improved due to the still presence of large particles which concentrate the stresses during tension tests and cause the sample breaks.

3.5 Rheology

The viscoelastic behaviour of neat PA5.10 and composites were investigated in order to evaluate the complex viscosity (η*) of the system. Figure 6 displays the logarithmic dependence of η* versus the angular frequency. Neat PA5.10 approached a constant value in the Newtonian plateau of 200 Pa•s. The addition of 20 wt.% of RHA or 5 wt.% of CL exhibited a higher viscosity than neat PA5.10 all over the investigated frequency range. These results can be explained in terms of restricted mobility of the polymer melt due to the

interaction between the polymer chains and filler in the melt [42]. These results also exclude an extensive degradation of the matrix during the processing since the viscosity is increased. However, it should be emphasized that PA5.10_20S shows a lower increase in viscosity compared to PA5.10_5C that may be due to the larger size of the RHA filler and its low aspect ratio geometry but also to possible partial degradation of the matrix which would also explain the mechanical properties reduction.

On the other hand, the complex viscosity of the PA5.10_10S5C composite is substantially different from the previous ones. The contemporaneous presence of the CL and the RHA produces a synergistic effect on the complex viscosity by creating a strong shear-thinning behaviour without a Newtonian plateau. This fact brings the complex viscosity to reach a value about two orders of magnitude higher than PA5.10_5C and PA5.10_20S confirming a strong interaction between the two fillers that creates a consistent solid-like structure at low shear rates. The high viscosity and consequently low chain mobility bring benefits in the thermo-mechanical properties of the material.

3.6 Crystallinity studies with DSC and XRD analyses

Continuing the exploration of the reasons that lead to the variation of the mechanical and thermo-mechanical properties of the composites, the crystallinity of the matrix was investigated with two characterization techniques. The DSC is used to evaluate a variation in crystallinity and XRD to evaluate a change in the crystalline phase and crystallites size.

The first heating scan in the DSC is important to understand the crystallinity of the final product as well as a film or an injection moulded object.

The same crystallinity has been found for the PA5.10 and PA5.10_5C films namely around 27% (Table 4). The two different shaping process of film extrusion and injection moulding on the neat PA5.10 gave some little differences in the crystallinity (27 vs. 24%). The film

stretching allows reaching a high crystallinity to the material. RHA seems not to have a sensible influence on the DSC data of injection moulded samples (X_c=23%). Conversely, clay in joint action with RHA promotes the crystallization that reaches 27%.

To complete the study on the crystallinity of the composites, XRD analyses have been performed and reported in Figure 7. By this way, the crystal structure was identified and crystal dimension qualitatively supposed from the width of the peaks.

The XRD spectra show that the neat PA5.10 film presents the characteristic peak of γ crystalline form (strong single reflection at 2θ = 21.1°), as previously found for PA10.10 [23]. The addition of CL, that usually promotes the γ-form, slightly shift the peak at 21.6° and increase the intensity of the peak even if the percentage of crystallinity remains substantially unchanged according to the DSC data.

As far as RHA is concerned, it is mainly composed of silica (generally >95%) revealing a peak in the XRD analysis at 21.9° as reported in the literature for such by-product and due to crystobalite [43]. This characteristic peak is still present without significant modifications in the composites PA5.10_20S and PA5.10_10S5C. However, in these latter composites, another peak at 21.2° appears. This second peak is due to the crystalline phase of PA5.10, newly in the γ form as in the neat PA5.10 (peak at 20.9°). Comparing the peak due to the PA5.10, the RHA clearly changes its appearance, making it very narrow and thus composed of more ordered and bigger crystals.

The increase in the crystallites size is due to the nucleating effect of the RHA and it is a plausible explanation for the registered significant increase in the thermo-mechanical properties. However, there is no increase in the crystallinity amount of the material.

It seems that in the PA5.10_10S5C sample a really low intense peak at around 20° is raised instead of the only γ crystalline phase. Such peak is due to a different PA crystalline phase, probably the α phase [44].

Summing up, the significant enhancements in the mechanical and thermo-mechanical properties of PA5.10_5C10S with respect to the other composites can be first attributed to the reinforcing effect of the CL and RHA. The crystallinity amount in the composite was essentially not deeply altered by the presence of the fillers but the crystal dimensions are increased by the inorganic filler presence.

Furthermore, the synergistic improvements obtained in the micro-nano composites can be partly explained by a small increase in crystallinity and by the appearance of a new crystalline phase (α) which is considered to be more stable, resistant and with a lower strain at break than the γ [45].

3.7 Pukanszky's model application

To better characterize the efficiency of transferring stresses from the matrix to the fillers also in the case of micro-nano composite, Pukanszky's model was applied to the different composites exploiting the tensile strength at yield point (σ_y) as suggested from the literature [6, 35, 46, 47].

Theoretically, the plot of the reduced stress at yield in logarithm form ($\log \sigma_{red}$) as a function of the volumetric fraction (φ) gives a straight line typical of each filler in a matrix. The line slope is the quantitative value (B factor) that correspond to the load carrying capability of each filler. The data obtained from the composites containing only CL are plotted with the half-filled marker in Figure 8, RHA data are plotted in the same figure with the empty marker and the data of the composites with both fillers with the filled marker. In addition to the plot, the calculated interpolation lines as dotted curves and previous research data with other bio-PAs [6, 23] were shown.

As already commented by strength data, it is evident from the reported B factor in Figure 8 that the best stress transfer is achieved by using the CL (14.95) and the worst with RHA

(3.07). The contemporary use of CL and RHA gave an intermediate result (4.52) that is slightly lower than what was reported for PA6.10 and PA10.10 [23]. Thus, in PA5.10 the CL is not able to increase the adhesion as much as in the case of the other two studied bio-PAs despite the best performance reported when it is single used. Probably the production process, film extrusion versus injection moulding, has a significant influence on the ability to orient and disaggregate the CL platelets that influence the load-transfer ability.

Pukanszky's model could be useful for the evaluation of the CL extent of exfoliation. Indeed, SEM analyses and XRD patterns can only show the intercalated or aggregated part of the fillers but are not able to highlight a possible exfoliation of clay layers. Thanks to Pukanszky's factor is possible to quantitatively evaluate the extent of exfoliation with Equation 2.

The best result reported in the literature was 11.7% of exfoliation in PA6 matrix [48] and in a previous study with PA10.10, a CL exfoliation degree of 4.5% was reached. The PA5.10 yielded an exfoliation rate of 6.8%, significantly higher than that obtained with PA10.10 [23]. As expected, the more polar matrix is able to exfoliate more the modified clay resulting in the best mechanical and barrier properties. On the other hand, CL in the combined system seems to have a limited exfoliation especially in PA5.10 matrix confirmed by the lower B factor.

4. Conclusions

The goal of the present research activity was to study new composite systems based on bio-PA5.10 mainly to increase the barrier properties in the thin film and the thermo-mechanical properties in bulk objects. These objectives were assessed by melt compounding rice husk ash (RHA) and/or modified clay (CL) and then shaping to the final form with industrialized machines. The resulting tensile mechanical properties in the film containing CL gave 45% of modulus and 36% of yield stress increase with respect to the neat PA5.10. Pukanszky's model was exploited to evaluate the filler-matrix interactions revealing that the CL has the best

interaction with PA5.10 with respect to other bio-PAs and reach a calculated exfoliation degree of 6.8%. Considering the barrier properties, the CL was able to decrease the oxygen permeability to less than half concerning neat PA5.10.

In the injection moulded samples, 20 wt.% of RHA induced significant improvement in Young's modulus (+53%) while a slight reduction in the yield and maximum tensile strength (-2% and -16%, respectively) and a dramatic decrease in the deformation at break (-97%) with respect to the neat matrix. Such fact is due to a low filler interaction with the matrix and a partial reduction of the polymer chain length. To reach more balanced properties, the reduction of RHA amount to 10 wt.% with the simultaneous addition of 5 wt.% of CL were investigated. The stress-strain analyses showed that the composite with both RHA and CL induced the best improvement in the elastic modulus (+84%) as well as in the tensile strength (+9%).

The DMTA data demonstrated that the addition of RHA caused a consistent increase (+46°C) in the heat deflection temperature (HDT) compared to the neat PA5.10 matrix (62°C). Furthermore, the simultaneous presence of RHA and clay provided the best result reaching an extraordinary HDT of 131°C. These results are comparable with different studies present in the literature with other bio-PA proving the possibility to develop also this matrix.

The two fillers investigated can therefore be used alone or together combined in PA5.10 for functional purposes in a sustainable scenario.

Acknowledgements

The Authors would like to thank Mr. Alberto Cisternino for the compounding of the materials.

Table 1. Codes and nominal compositions of melt-blended PA5.10-based samples.

Sample	PA5.10 [wt.%]	CL [wt.%]	RHA [wt.%]
PA5.10	100.0	-	-
PA5.10_5C	95.0	5.0	-
PA5.10_20S	80.0	-	20.0
PA5.10_10S5C	85.0	5.0	10.0

Table 2. Thickness and Oxygen Permeability (OP) of film extruded neat PA5.10 and PA5.10_5C.

Permeability at 50% R.H.	Thickness [mm]	OP [cm^3*mm/m^2*day*atm]
PA 5.10	0.10±0.02	3.7±0.4
PA 5.10_5C	0.21±0.01	1.8±0.1

Table 3. Tension test data and HDT of PA5.10-based composites.

		Extruded film		Injection moulded		
		PA5.10	5C	PA5.10	20S	10S5C
Stress-strain analysis at 23°C	E [GPa]	1.39±0.24	2.16±0.08	1.49±0.04	2.29±0.04	2.76±0.06
	ΔE [%]*	-	+45	-	+53	+84
	σ_y [MPa]	37.5±1.7	51.2±2.3	52.1±0.4	51.0±0.3	57.1±0.7
	$\Delta \sigma_y$ [%]*	-	+36	-	-2	+9
	σ_{max} [MPa]	62.3±3.7	67.2±3.0	60.9±4.0	51.0±0.3	57.0±0.7
	$\Delta \sigma_{max}$ [%]*	-	+8	-	-16	-6
	ε [%]	221±9	90±6	332±18	10±1	5±1
HDT from DMTA	1.81 MPa [°C]**	-	75	62	108	131

* Δ = (matrix property - composite property) / matrix property ** Calculated with E' data from DMTA

Table 4. DSC data of all PA5.10-based materials

Sample	ΔH_{sr} [J/g]	ΔH_m [J/g]	ΔH_{m-sr} [J/g]	X_c [%]
PA5.10film	2.5	70.2	67.7	27.7
PA5.10_5Cfilm	3.9	65.9	65.3	26.7
PA5.10	3.9	63.5	59.6	24.4
PA5.10_20S	3.5	48.3	56.0	23.0
PA5.10_10S5C	3.0	59.5	66.5	27.2

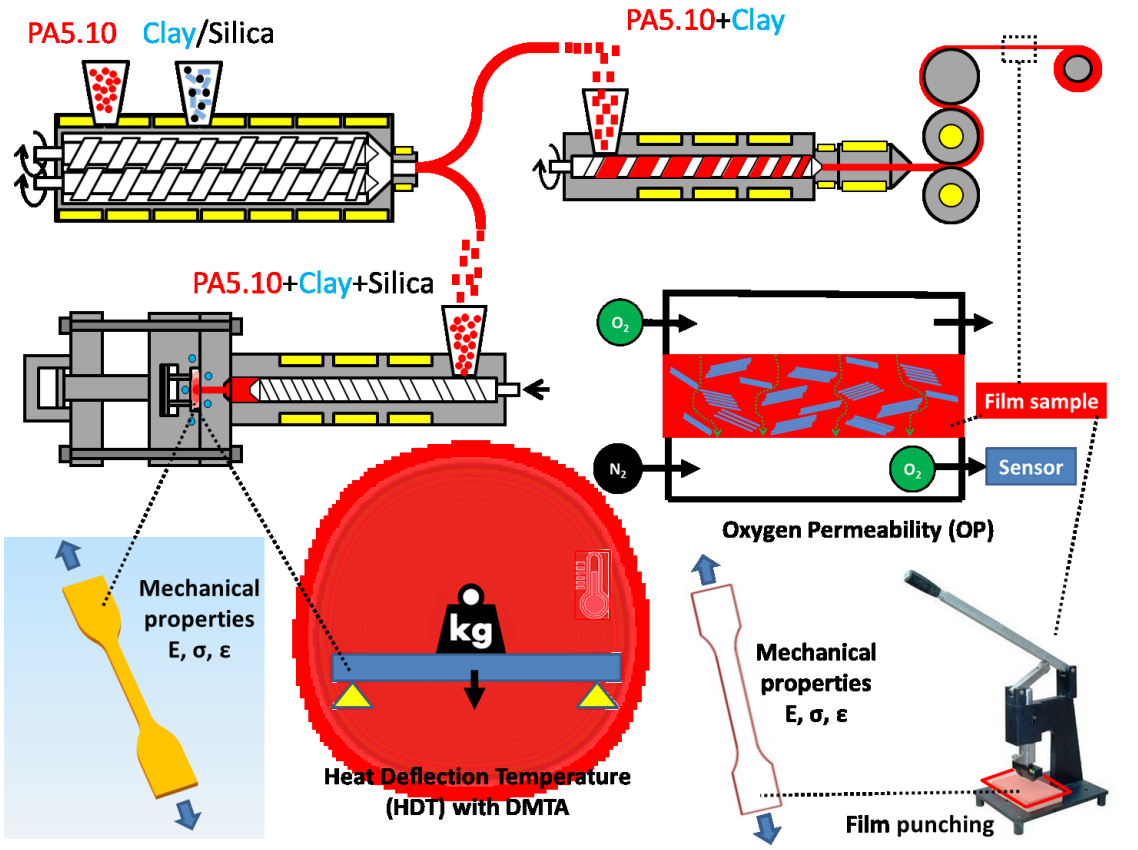

Figure 1. Schematic outline of material processing and testing

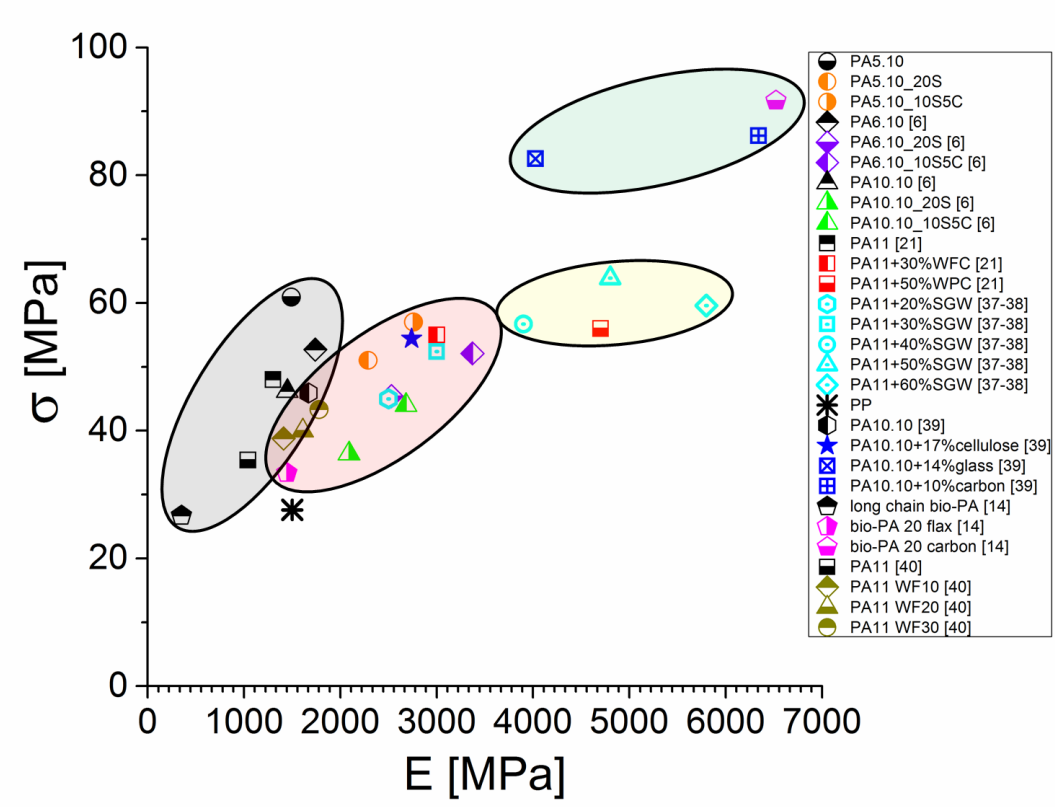

Figure 2. Tensile modulus (E) versus strength (σ) of bio-PAs and composites.

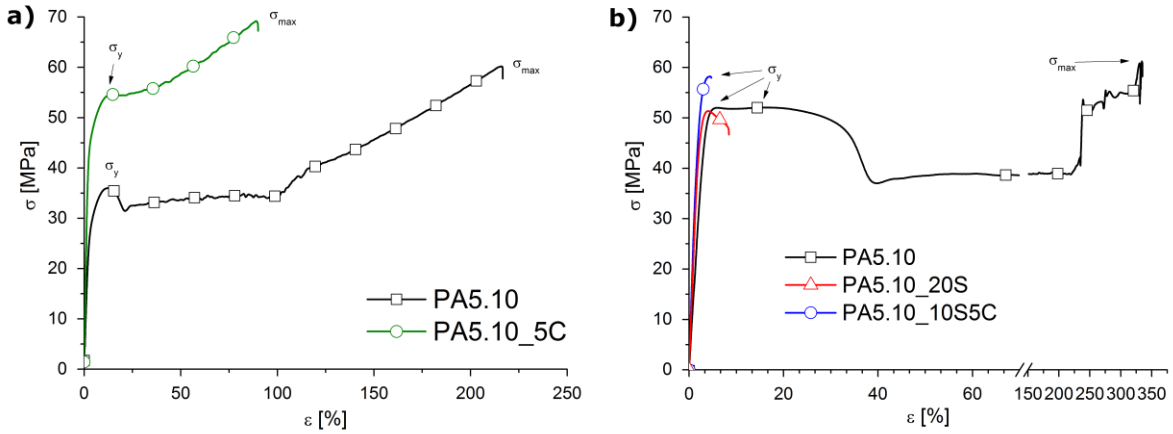

Figure 3. Representative stress-strain curves of: a) PA5.10 and PA5.10_5C in thin film, b) PA5.10-based composites obtained with injection moulding.

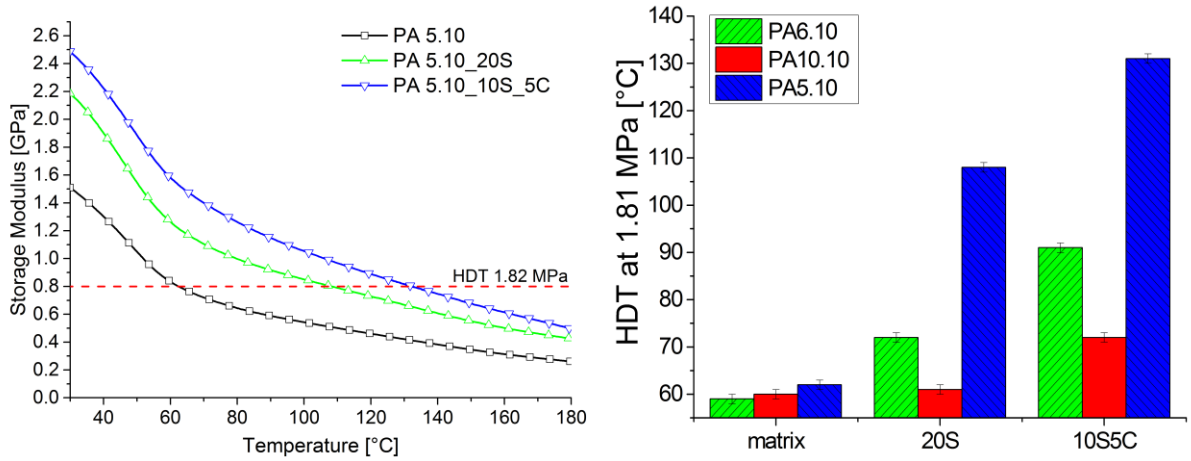

Figure 4. Storage modulus E' as a function of the temperature of PA5.10-based composites with HDT dotted line and HDT comparison with other bio-PAs.

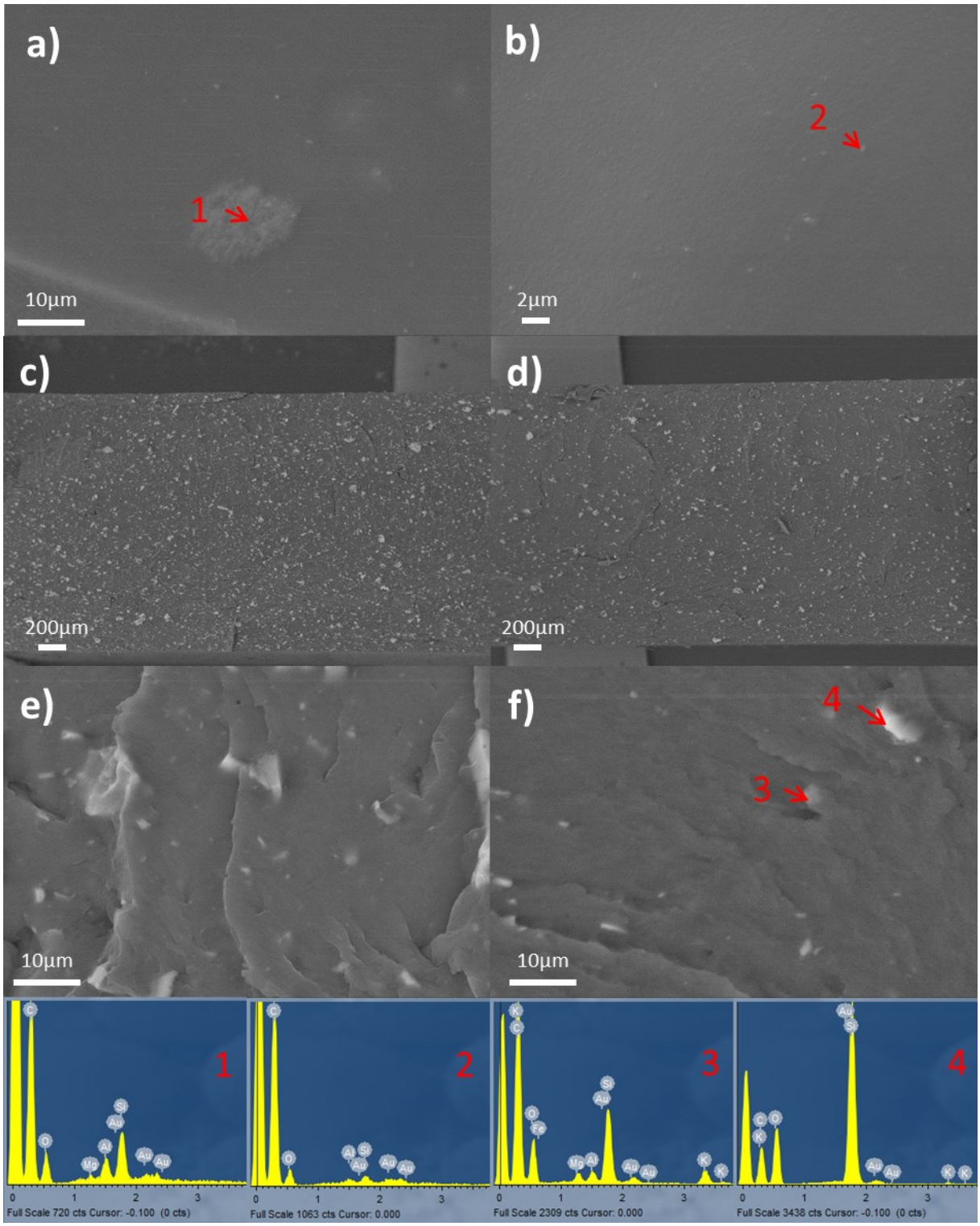

Figure 5. SEM cross sections of: PA5.10_5C (a), (b), PA5.10_20S (c), (e) and PA5.10_10S5C (d), (f).

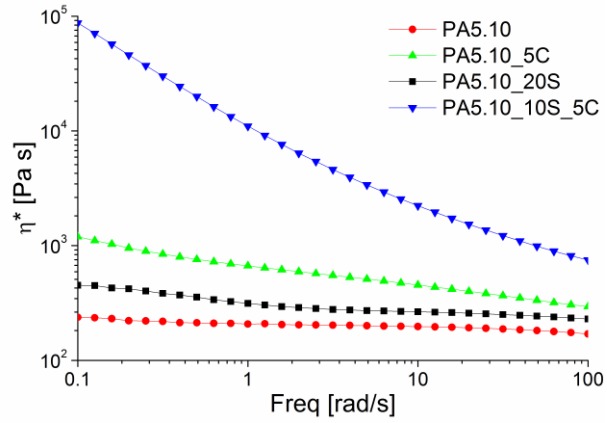

Figure 6. Complex viscosity (η*) of PA5.10 and composites.

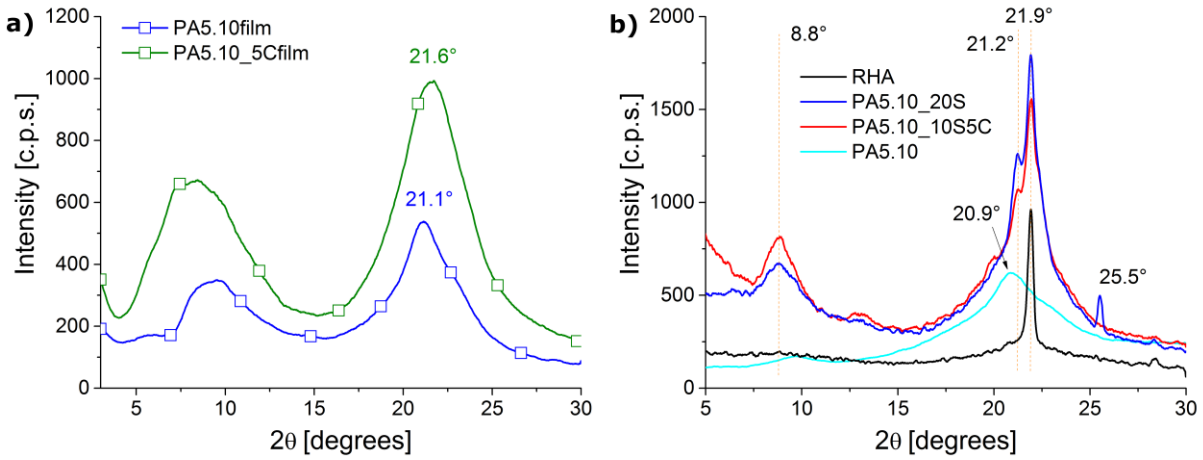

Figure 7. XRD of film extruded PA5.10 and PA5.10_5C (a) and injection moulded samples and RHA (b).

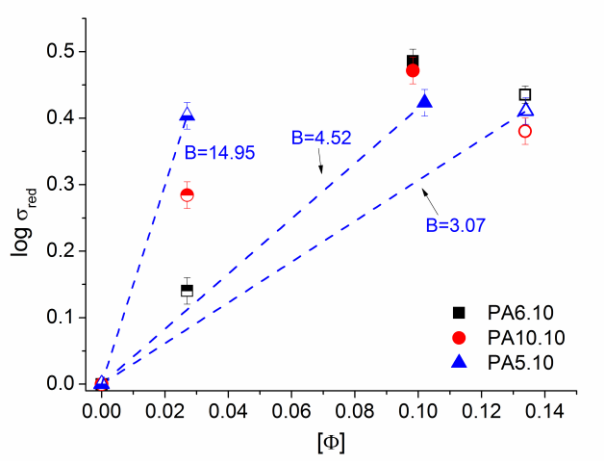

Figure 8. Reduced stress data (log σ_{red}) of PA5.10-based composites (sample with only CL are plotted with half-filled marker, 20S with the empty marker and 10S5C with fully filled marker) with fitting dotted lines according to Pukanszky's model and data from previous studies [6, 23].

References

[1] EB Association (2018),
[2] J Pagacz, KN Raftopoulos, A Leszczyńska, K Pielichowski (2016) Journal of Thermal Analysis and Calorimetry 123: 1225. Doi:10.1007/s10973-015-4929-x
[3] DA Ruehle, C Perbix, M Castaneda, et al. (2013) Polymer 54: 6961. Doi:10.1016/j.polymer.2013.10.013
[4] A Al-Mulla (2009) International Journal of Polymer Analysis and Characterization 14: 540. Doi:10.1080/10236660903086136
[5] D Battegazzore, J Alongi, G Fontaine, A Frache, S Bourbigot, G Malucelli (2015) RSC Advances 5: 39424.
[6] D Battegazzore, O Salvetti, A Frache, N Peduto, A De Sio, F Marino (2016) Compos Part a-Appl S 81: 193. Doi:10.1016/j.compositesa.2015.11.022
[7] M Feldmann, AK Bledzki (2014) Composites Science and Technology 100: 113.
[8] MQ Yan, HJ Yang (2012) Polymer Composites 33: 1770. Doi:10.1002/pc.22318
[9] PFH Harmsen, MM Hackmann, HL Bos (2014) Biofuels, Bioproducts and Biorefining 8: 306. Doi:10.1002/bbb.1468
[10] PA Wilbon, F Chu, C Tang (2013) Macromolecular Rapid Communications 34: 8. Doi:10.1002/marc.201200513
[11] M Winnacker, B Rieger (2015) ChemSusChem 8: 2455.
[12] M Winnacker, B Rieger (2016) Macromolecular Rapid Communications 37: 1391. Doi:10.1002/marc.201600181
[13] HT Kim, KA Baritugo, YH Oh, et al. (2018) ACS Sustainable Chemistry and Engineering 6: 5296. Doi:10.1021/acssuschemeng.8b00009
[14] S Kuciel, P Kuzniar, A Liber-Knec (2012) Polimery 57: 627. Doi:DOI 10.14314/polimery.2012.627
[15] A Leszczyńska, K Stafin, J Pagacz, et al. (2018) Industrial Crops and Products 116: 97. Doi:10.1016/j.indcrop.2018.02.022
[16] S Kind, C Wittmann (2011) Applied Microbiology and Biotechnology 91: 1287. Doi:10.1007/s00253-011-3457-2
[17] MM Hasan, Y Zhou, H Mahfuz, S Jeelani (2006) Materials Science and Engineering: A 429: 181. Doi:10.1016/j.msea.2006.05.124
[18] ZJ Liu, PL Zhou, DY Yan (2004) Journal of Applied Polymer Science 91: 1834. Doi:DOI 10.1002/app.13336
[19] E Picard, A Vermogen, JF Gerard, E Espuche (2007) Journal of Membrane Science 292: 133. Doi:10.1016/j.memsci.2007.01.030
[20] F Sadeghi, M Fereydoon, A Ajji (2013) Advances in Polymer Technology 32: E53. Doi:10.1002/adv.20270
[21] P Zierdt, A Weber (2015) Materials Science ForumTrans Tech Publ,
[22] D Battegazzore, A Frache, T Abt, ML Maspoch (2017) in Fractura SdGEd (ed)XXXIV ENCUENTRO DEL GRUPO ESPAÑOL DE FRACTURASecretaría del Grupo Español de Fractura, Santander
[23] D Battegazzore, A Sattin, ML Maspoch, A Frache (2018) Polymer Composites. Doi:10.1002/pc.25056
[24] S Turmanova, S Genieva, L Vlaev (2012) International Journal of Chemistry 4. Doi:10.5539/ijc.v4n4p62
[25] DS Chaudhary, MC Jollands, F Cser (2004) Advances in Polymer Technology 23: 147. Doi:10.1002/adv.20000
[26] EP Ayswarya, KF Vidya Francis, VS Renju, ET Thachil (2012) Materials & Design 41: 1. Doi:10.1016/j.matdes.2012.04.035

[27] W Arayapranee, N Na-Ranong, GL Rempel (2005) Journal of Applied Polymer Science 98: 34. Doi:10.1002/app.21004
[28] S Siriwardena, H Ismail, US Ishiaku (2003) Journal of Reinforced Plastics and Composites 22: 1645. Doi:10.1177/073168403027619
[29] MYA Fuad, Z Ismail, MS Mansor, ZAM Ishak, AKM Omar (1995) Polymer Journal 27: 1002. Doi:DOI 10.1295/polymj.27.1002
[30] MT Takemori (1979) Polym Eng Sci 19: 1104. Doi:DOI 10.1002/pen.760191507
[31] Y Khanna, W Kuhn (1997) Journal of Polymer Science Part B: Polymer Physics 35: 2219.
[32] A Ciaperoni, A Mula (2001) Pacini Editore, Pisa, Italy: 154.
[33] B Pukanszky (1990) Composites 21: 255. Doi:Doi 10.1016/0010-4361(90)90240-W
[34] D Battegazzore, Noori, A., Frache A. (2018) Journal of Composite Materials.
[35] L Százdi, A Pozsgay, B Pukánszky (2007) European Polymer Journal 43: 345. Doi:https://doi.org/10.1016/j.eurpolymj.2006.11.005
[36] J Atkinson (1993) Concise encylopedia of polymer processing & applications. Ed. Patrick J. Corish, Pergamon Press, Pergamon Press, Oxford
[37] H Oliver-Ortega, F Julian, FX Espinach, Q Tarrés, M Ardanuy, P Mutjé (2019) Journal of Cleaner Production 226: 64. Doi:10.1016/j.jclepro.2019.04.047
[38] H Oliver-Ortega, LA Granda, FX Espinach, JA Mendez, F Julian, P Mutjé (2016) Composites Science and Technology 132: 123. Doi:https://doi.org/10.1016/j.compscitech.2016.07.004
[39] AA Nikiforov, SI Vol'fson, NA Okhotina, R Rinberg, T Hartmann, L Kroll (2017) Russian Metallurgy (Metally) 2017: 279. Doi:10.1134/s0036029517040152
[40] S Armioun, S Panthapulakkal, J Scheel, J Tjong, M Sain (2016) Journal of Applied Polymer Science 133. Doi:10.1002/app.43595
[41] D Battegazzore, S Bocchini, J Alongi, A Frache (2014) RSC Advances 4: 54703.
[42] A Gupta, W Simmons, GT Schueneman, D Hylton, EA Mintz (2017) ACS Sustainable Chemistry & Engineering 5: 1711.
[43] VP Della, I Kühn, D Hotza (2002) Materials Letters 57: 818.
[44] P Villaseñor, L Franco, J Subirana, J Puiggali (1999) Journal of Polymer Science Part B: Polymer Physics 37: 2383.
[45] R Seguela (2005) Journal of Macromolecular Science Part C: Polymer Reviews 45: 263.
[46] J Móczó, B Pukánszky (2008) Journal of Industrial and Engineering Chemistry 14: 535.
[47] J Hári, F Horváth, K Renner, J Móczó, B Pukánszky (2018) Polymer Testing 72: 178.
[48] J Shelley, P Mather, K DeVries (2001) Polymer 42: 5849.